Lattice Curvature in Nearly Perfect Silicon Crystals

R. Bubáková and Z. Trousil

Institute of Solid State Physics, Czech. Acad. Sci., Prague

(Z. Naturforsch. **28 a**, 1199–1204 [1973]; received 18 May 1973)

Dedicated to Professor Dr. G. Borrmann on his 65th birthday

Deviations from Friedel's law in the case of anomalous transmission of X-rays have been estimated in as-grown silicon crystals.

The results of measurements on a double crystal spectrometer agree with the dynamical theory of elastically deformed crystals. Using this theory, we have obtained information about growth deformation in crystals containing a small number of dislocations or in dislocation-free ones. Radii of curvature of crystal lattice planes of the order of km, orientation differences of the order of 0.1″ and relative changes of lattice constants of the order of 10^{-3}% have been estimated.

Dislocation loops were observed at the boundary between the dislocation-free and the distorted part of the crystal.

Introduction

It is well known that anomalous transmission of X-rays, observed first by Borrmann [1], is sensitive to deformations of lattice planes due to mechanical stresses [2] or due to temperature gradients [3]. It has been reported that Friedel's law loses its validity in the case of anomalous transmission both at low angle boundaries [4] and in the presence of small local defects in crystals [5].

On the other hand the results of the dynamical theory of X-ray diffraction, extended to elastically deformed crystals [6, 7], experimentally proved in [8], make it possible to determine deformations of crystal lattices from deviations from Friedel's law.

This led us to try to measure the deviations from Friedel's law in the case of anomalous transmission of X-rays in as-grown nearly perfect Si crystals in order to determine small long-range growth deformations of their crystal lattice. The aim of this experimental work was to detect the curvature of lattice planes parallel to the growth axis and eventually to find variations of this curvature with changing distance from this axis. Another point of interest was to examine the differences in this variation at the origin and at the end of the investigated crystals. For this purpose nearly perfect silicon crystals were chosen grown in the ⟨112⟩ direction. Our experiments have shown so far that dislocations in these crystals are oriented preferably parallel to the growth axis.

All measurements were carried out on a double-crystal spectrometer.

Crystals used in Experiments

The silicon crystals were prepared by a special technique [9]. Its technology will be published later.

The investigated crystal specimens were cut from four crystals, the growth axis of which was $[11\bar{2}]$ and selected with respect to etch figures and growth conditions:

I. The first crystal contained 15 dislocations. Eight of them were near to the crystal origin arranged in a low angle boundary, perpendicular to (111) lattice planes.

II. The second crystal was grown initially as pure and dislocation-free. In a later stage carbon was added to the atmsophere in which the crystal was growing. The first approximately 2 cm long part of this crystal was grown without any apparent change. Suddenly a great number of dislocations appeared and the last part of the crystal was very imperfect.

III. Initially the third crystal was dislocation-free but it might have contained small concentrations of oxygen and carbon. However the optical absorption in the region of 9 μ in the infrared was not observed. Although the conditions during the growth were not changed, a large number of dislocations appeared suddenly in a later stage of growth.

IV. The fourth crystal contained 22 dislocations. Twenty of them were arranged parallel to the (111) plane as can be seen in the cross-section of the specimen in Figure 1.

All these crystals were cylinder like with a diameter of 10.5 – 12 mm. A narrow strip of natural (111) face appeared on the cylindrical part of all

Reprint requests to R. Bubáková, Institute of Solid State Physics, Academy of Siences, 162-53 *Prague 6*, Czechoslovakia.

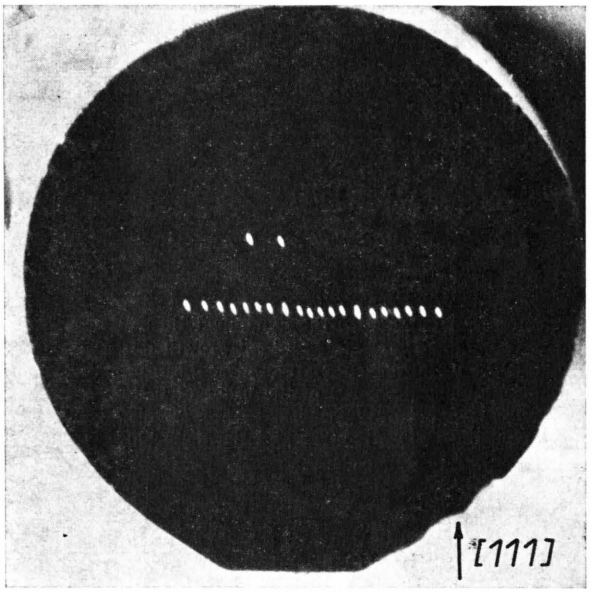

Fig. 1. Etch figures on a $(11\bar{1})$ cross section of the silicon crystal IV. The average spacing between the dislocations is 0.24 mm.

four crystals. The planes as observed from the surface of the mentioned strip were indexed (111), the opposite side of the same planes is referred to as $(\bar{1}\bar{1}\bar{1})$.

Crystal specimens I and II were plates with $(1\bar{1}0)$ surfaces parallel to the growth axis as can be seen from Figure 2 a. Specimens of the form of parallelepipeds from crystal III and IV were cut with faces parallel to (111) and $(1\bar{1}5)$ planes, as shown on Figure 2 b.

The faces of the specimens were ground and polished to within 1° from the given orientation and then etched in a mixture of $1\,HF + 5\,HNO_3$ to remove the remaining surface damage. The thicknesses D_0 of the specimens are indicated in Table 1.

Measurements

An X-ray double-crystal spectrometer in $(n, -n)$ position was employed. Characteristic MoKα radiation (focus 1×1 mm^2) impinging on the first crystal had to pass a cylindrical collimator of diameter 2 mm.

For the sake of better reproducibility of the alignment of diffracting planes [10] symmetric Bragg-case reflexions was preferred for the first silicon crystal, which was pure and dislocation-free. The second crystal (the investigated specimen) was in the symmetric Laue position. A slit 2 mm wide and 3 mm

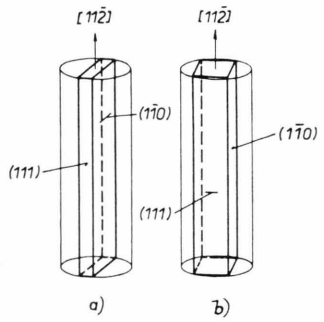

Fig. 2. Orientation of specimens cut from silicon crystals grown in $[11\bar{2}]$ direction.

high was located between both crystals, limiting the vertical divergence of the beam and allowing only the MoK$\alpha_{1,2}$ radiation to pass. The diffracted beam was detected by a scintillation counter with a pulse height discriminator so that there was no trouble with higher harmonics from the first crystal.

The deviation from Friedel's law was found by comparing the maxima of the $(h\,k\,l)$ and $(\bar{h}\,\bar{k}\,\bar{l})$ rocking-curves, obtained by measuring the diffracted intensity when the second crystal was rotated. The curvature of the diffracting planes (111) in the specimens I and II and of the planes (111) and $(2\bar{2}0)$ in the specimens III and IV was investigated in this way. To relate the deviations from Friedel's law to the distance from the growth axis, the investigation was repeated whilst shifting the specimen horizontally stepwise from one edge to the other. In all cases both the intensities of the anomalously transmitted direct and reflected beams were measured.

Results

The results of the measurements obtained with the specimens I and III are indicated in Figure 3. The maxima of the rocking-curves are plotted as a function of the horizontal shift of the specimen from one border to the other. Each point represents the mean value of the maxima (in pulses per 1 min of time) of 10 rocking-curves obtained in the same position of the specimen. As can be seen from Fig. 3, the intensities of both direct beams in the pairs $R_0(111)$; $R_0(\bar{1}\bar{1}\bar{1})$ and $R_0(\bar{2}20)$; $R_0(2\bar{2}0)$, respectively, were nearly the same in each position of the specimen. Moreover the variation of the intensities of these pairs of beams was relatively small, when the specimen was shifted horizontally.

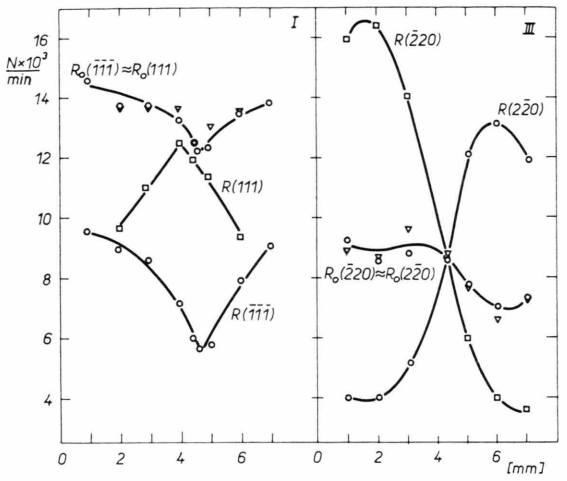

Fig. 3. The validity of Friedel's law for different horizontal shifts of specimens I and III. $R(hkl)$ — reflected beam, $R_0(hkl)$ — direct beam. Maximum values of intensity (in pulses per 1 min) □ ▽ hkl, ○ $\bar{h}\bar{k}\bar{l}$ diffraction.

The reflected beams behaved in quite a different way. The maxima of the rocking curves $R(111)$ and $R(\bar{1}\bar{1}\bar{1})$ or $R(\bar{2}20)$ and $R(2\bar{2}0)$, respectively, were reproducibly dependent on the specimen's position as can be seen from Figure 3. The greatest deviations from Friedel's law are to be found in the central part of specimen I (i. e. near the growth axis). On the other hand these deviations are high at the borders of the specimen III (i. e. near te surface of the crystal III).

For all specimens we found $R_0(h\,k\,l) = R_0(h\,k\,l)$ within $\pm 4\%$ (probable error). To eliminate an eventual long time instability of the apparatus each value of $R(h\,k\,l)$ was related to the corresponding $R_0(h\,k\,l)$. As functions of the specimens positions we have plotted in the upper parts of Figs. 4 and 5 b the results for $R/R_0(h\,k\,l)$ taken from Fig. 3, and in Fig. 5 a the results for R/R_0 obtained by diffraction on (111) and $(\bar{1}\bar{1}\bar{1})$ in crystal III. The directions of the X-ray beams in the specimens are shown on the right hand sides of Figures 4 and 5.

The results presented in Figs. 4 and 5 are obtained on all four specimens. In I and IV, there was practically no difference in R/R_0 between positions of the crystal near the origin and in a distance 2 cm

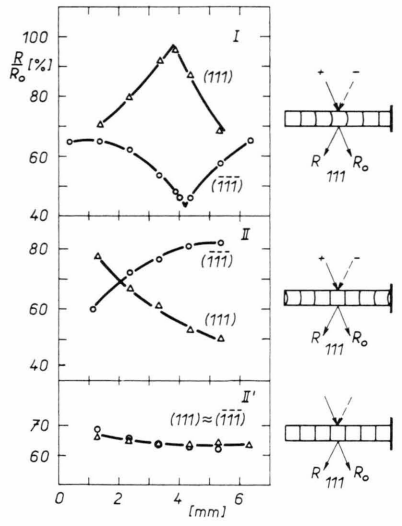

Fig. 4. Friedel's law validity for different horizontal shifts of specimen I and II. R/R_0 — ratio of intensity maximum of reflected and direct beam. On the right hand side the schematic X-ray beam orientation and deformation of lattice planes is indicated.

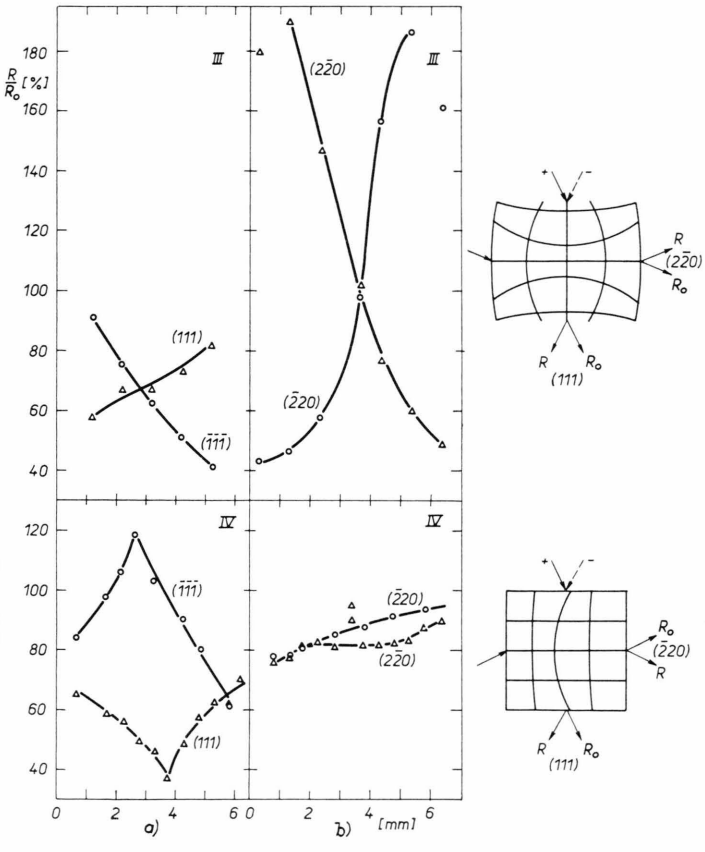

Fig. 5. Analogy to Fig. 4 for specimens III and IV.

below the origin (measured after shifting the specimen vertically). Figure 4/I and Fig. 5/IV indicate the behaviour of specimens I and IV for these two positions of the crystal. On the other hand the results of II and III, shown in Figs. 4/II and 5/III, are only related to those parts of the specimen, where the dislocations were suddenly generated. The upper edge of the beam was about 5 mm far from dislocation loops. Near the origin of the crystal no deviations from Friedel's law were found both in II and in III. The results obtained in this part of specimen II are shown in Figure 4/II′.

These results were reproducible even when repeated after one year.

The generated dislocation – loops on the boundary between the dislocation – free and the distorted part of crystal III can be seen on Figure 6.

Fig. 6. Dislocation loops on the boundary between dislocation-free and distorted part of silicon specimen III. Borrmann's case topography on a double crystal spectrometer [$R(2\bar{2}0)$ diffraction, the area shown on the figure is 1.23 mm×1.88 mm].

Discussion

The experimental result $R_0(h\,k\,l) = R_0(\bar{h}\,\bar{k}\,\bar{l})$ agrees with that of the dynamical theory for thick elastically deformed crystals [6, 7].

From this theory the following relation results

$$\xi_+^{\,2} = \frac{1}{\xi_-^{\,2}} \tag{1}$$

in which

$$\xi_+^{\,2} = \left(\frac{R}{R_{0\mathrm{R}}}\right)(h\,k\,l) \quad \text{and} \quad \xi_-^{\,2} = \left(\frac{R}{R_{0\mathrm{R}}}\right)(h\,k\,l). \tag{2}$$

Here R and $R_{0\mathrm{R}}$ indicate the maximum reflexion coefficient and the related transmission coefficient respectively. We estimated in our experiments R and the maximum transmision coefficient R_0. Both in ideal [11] and in elastically deformed crystals [7] R and R_0 do not appear simultaneously in the same angular position of the crystal. Due to this fact is $R_{0\mathrm{R}} \neq R_0$. Introducing $R_{0\mathrm{R}} = K R_0$ in relation (1) and (2) we obtain

$$\left(\frac{R}{K R_0}\right)(h\,k\,l) = \left(\frac{K R_0}{R}\right)(h\,k\,l). \tag{3}$$

To find the relation for K, we calculated the extremum values R and R_0 of the reflexion and transmission coefficients. In this calculation we neglected the contribution of the heavily damped mode. We found the approximate relations

$$\Delta\eta \approx 2\,\gamma_0/(\mu\,D_0\,\varepsilon + 2\,\gamma_0)$$

for the angular distance between the positions of R and R_0 and also

$$K \approx -\Delta\eta + 1 + \tfrac{1}{2}\Delta\eta^2 \tag{4}$$

were $\eta = \frac{1}{2}(\xi - 1/\xi)$, γ_0 is the direction cosine of the incident wave in the symmetrical Laue case, $\varepsilon = \chi_{ih}/\chi_{i0}$, where χ_{ih} and χ_{i0} are the $h\,k\,l$ and 000 Fourier coefficients of the imaginary part of the electric susceptibility respectively.

For silicon crystals and MoKα radiation

$$\gamma_{111} = 0.9935 \quad \text{and} \quad \gamma_{220} = 0.9837.$$

Using [12] and $e_{111}^{-M} = 0.989$ and $e_{220}^{-M} = 0.970$, we found $\varepsilon_{111}^{\perp} = 0.698$ and $\varepsilon_{220}^{\perp} = 0.967$. Relation (4) gives $K_{111} \approx 0.77$ for $\mu D_0(111) = 8.25$ for specimen II and $K_{220} \approx 0.88$ for $\mu D_0(220) = 13.8$ for specimen III.

The value of K, determined from experimental results using relations (3) for specimen II, 111 and $\overline{111}$ diffractions, is $K = K_{\mathrm{i}} = 0.65 \pm 0.03$ and for specimen III, $\bar{2}20$ and $2\bar{2}0$ diffractions, is $K = K_{\mathrm{i}} = 0.94 \pm 0.04$. K_{i} indicates the value related to that part of the specimen in which no deviation from Friedel's law was observed and K that part in which the highest deviation from Friedel's law was found.

Both experimental values of K are in qualitative agreement with the corresponding approximate theoretical values. Relation (3) is valid for all experimental results [13].

In order to check the deformation of the investigated crystals, we calculated the smallest radius r of curvature, the greatest angular deviation α of diffracting planes and the relative change of the lattice

Table 1. D_0 is the thickness of the specimens, μ_0 the linear absorption coefficient, (hkl) the indices of diffracting planes, $(R/R_0)\,(hkl)$, $(R/R_0)\,(hkl)$ the ratios of intensity maximum of reflected and transmitted beams (exp. values), r the smallest radius of curvature, α the greatest angular deviation of diffracting lattice planes, $\Delta d/d$ their relative change of lattice constant.

Specimen	D_0 cm	$\mu_0 D_0$	(hkl)	$\frac{R}{R_0}(hkl)$ %	$\frac{R}{R_0}(hkl)$ %	r km	α sec	$\frac{\Delta d}{d}\cdot 10^5$
I	0.53	7.95	111	96	45	1.9	0.29	1.2
II	0.55	8.25	111	49.5	82	3	0.19	0.8
III	0.95	14.25	111	82	41.5	3.8	0.26	1.1
	0.92	13.8	220	190	46.5	2.5	0.37	0.95
IV	0.75	11.25	111	37	119	1.7	0.45	1.8
	0.78	11.7	220	83	91	32	0.025	0.06

constant $\Delta d/d$ using experimental values of R/R_0, relations (2), (3) and the relation:

$$r = \frac{2\,D_0 \tan\Theta_B}{\chi_h}\,\frac{\xi}{\xi^2 - 1}$$

where Θ_B is the Bragg angle and χ_h a component of a Fourier series representing the density of scattering matter. The resulting values are shown in Table 1. The r values of II and III could be near to the critical radius for the generation of dislocations in a dislocation-free crystal lattice in this growth orientation.

Knowing the orientation of the incident beam it was possible to determine the sign of r in the specimen. The variation of r, corresponding to the variation in the values of R/R_0 is schematically shown in the cross-sections of the specimen in Figures 4 and 5.

Noteworthy is the deformation of the dislocation-free specimen III, found in the part of the crystal where dislocations originated. The systems of lattice planes, perpendicular to each other in the perfect crystal also remain perpendicular in the deformed state.

The results on Fig. 5/IV show a strong deformation of (111) planes near the axis of the specimen (radius of curvature 1.7 km). On the other hand the deformation of the $(1\bar{1}0)$ planes was nearly negligible. It is possible in the arrangement of dislocations shown in Fig. 1, that the (111) lattice planes have a fan-like deformation. Though these planes are not parallel, the beam behaves as if no strains were present [7].

For the specimen II we have tried to estimate the concentration of carbon atoms located in the silicon lattice near that part of the crystal where dislocations were generated. The highest relative change of (111) lattice constant gives the atomic concentration 24×10^{-6} (i. e. $1.2 \times 10^{18}/\mathrm{cm}^3$ of carbon atoms). This could be near to the critical value where the growth of dislocation-free crystals is still possible for a given stability of the growth conditions. The estimated value seems not to be in contradiction to the solubility value of $1.5 \times 10^{18}/\mathrm{cm}^3$ at 1402 °C found by diffusion of radioactive C in the Silicon lattice [14].

Conclusion

Examining the validity of Friedel's law by means of anomalous transmission of X-rays on chosen specimens, we have tried to detect the long-range growth deformation in nearly perfect silicon crystals.

The accuracy of this method seems to be sufficient for the measurement of lattice curvatures in crystals which are not quite pure but free of dislocations. Therefore the method should be important for the study of nearly perfect crystals. For example it could be used for the determination of the concentration of electrically inactive impurities, inhomogeneously distributed in a "pure crystal". Another field of interest could be the investigation of conditions for the generation of dislocations in dislocation-free crystals.

The authors would like to thank Dr. J. Čermák for his interest and clarifying discussions.

[1] G. Borrmann, Physik. Z. **42**, 157 [1941].
[2] L. P. Hunter, Proc. Kon. Ned. Akad. Wettensch. Amsterdam **B 61**, 214 [1958]. — B. Okkerse and P. Penning, Philips Res. Repts. **18**, 82 [1963].
[3] G. Borrmann and G. Hildebrandt, Z. Phys. **156**, 189 [1959]. — G. Hildebrandt, Z. Krist. **112**, 312, 340 [1959].
[4] R. Bubáková and J. Drahokoupil, VII. Int. Congress of IUC. Abst. A **15**, 2.6 [1966].

[5] B. W. Batterman and I. R. Patel, J. Appl. Physics **34**, 2716 [1963]. — G. H. Schwuttke and J. K. Howard, Appl. Physics **39**, 1581 [1968].
[6] N. Kato, J. Phys. Soc. Japan **18**, 1785 [1963]; **19**, 67, 971 [1964].
[7] P. Penning and D. Polder, Philips Res. Repts. **16**, 419 [1961].
[8] C. Malgrange, These de doctorat d'état es sciences Physique, Paris. — H. Hashizume and K. Kohra, J. Phys. Soc. Japan **29**, 805 [1970].
[9] Z. Trousil, Czech. J. Phys. **B 12**, 227 [1962].
[10] R. Bubáková, Czech. J. Phys. **B 12**, 695 [1962].
[11] M. v. Laue, Röntgen-Strahl-Interferenzen, Akad. Verlagsgesellschaft, Frankfurt (Main) 1960, S. 415.
[12] A. J. Guttmann and H. Wagenfeld, Acta Cryst. **22**, P3, 334 [1967].
[13] The widths at half maximum of all rocking-curves were found to be uniform to within $\pm 6\%$ so that the influence of instrumental distortion of the ratios R/R_0 was neglected.
[14] R. C. Newman and J. Wakefield, J. Phys. Chem. Sol. **19**, 230 [1961].

Bestimmung der Röntgen-Debye-Temperatur aus dem Borrmann-Effekt in Germanium

J. Ludewig

Fritz-Haber-Institut der Max-Planck-Gesellschaft, Berlin-Dahlem

(Z. Naturforsch. **28 a**, 1204—1213 [1973]; eingegangen am 21. April 1973)

Herrn Professor Dr. G. Borrmann zu seinem 65. Geburtstag gewidmet

Determination of the X-ray Debye Temperature in Germanium by Means of the Borrmann Effect

The anomal transmission of CuK radiation through "thick"' perfect crystal slices of Germanium is strongly temperature dependent. This temperature dependence was measured between 293 and 6 K in the (220) symmetric Laue case and used to evaluate the Debye temperature Θ_M. The well-known uncorrected value $\Theta'_M = 290$ K was obtained near room temperature. Taking into account TDS and Compton scattering in addition to the photoelectric absorption the corrected value $\Theta_M =$ 294 or 296 K was found, depending on the source of data. With decreasing temperature the corrected Θ_M increases slightly up to a maximum at very low temperatures, as predicted by Batterman and Chipman and by Salter.

1. Einführung

Der Borrmann-Effekt (die reduzierte Absorption interferierender Röntgen-Strahlung in nahezu perfekten Kristallen) erlaubt bekanntlich die Messung des minimalen Absorptionskoeffizienten $\mu_{\min}$, für den in einfachen Fällen, z. B. im Diamantgitter,

$$\mu_{\min}^{\perp} = \mu_0 (1 - |\chi_{ih}^{\perp}/\chi_{i0}|)/\cos\Theta_B \qquad (1)$$

gilt (μ_0 normaler, linearer Schwächungskoeffizient; Θ_B Bragg-Winkel). $\mu_{\min}$ hängt danach, außer von μ_0, im wesentlichen von der Größe $|\chi_{ih}^{\perp}/\chi_{i0}|$ ab. Diese besteht aus dem Imaginärteil verschiedener Fourier-Koeffizienten der dielektrischen Suszeptibilität und berücksichtigt verschiedene Arten der Wechselwirkung zwischen Strahlung und Kristallgitter. Beschränken wir uns auf Reflexe mit geradzahligen Laue-Indizes $h = \{h_1, h_2, h_3\}$ des Diamantgitters, so gilt in erster Näherung

$$|\chi_{ih}^{\perp}/\chi_{i0}| \approx D_h' \varepsilon_0^{\perp}. \qquad (2)$$

Sonderdruckanforderungen an Dr. J. Ludewig, Fritz-Haber-Institut der Max-Planck-Gesellschaft, *D-1000 Berlin 33*, Faradayweg 4—6.

Der Debye-Waller Faktor D_h trägt dem Einfluß der Gitterschwingungen auf die Absorption der Wellenfelder Rechnung, $\varepsilon_0^{\perp}$ der Photo-Absorption mit ihrer von D_h abweichenden Winkelabhängigkeit. Obwohl χ_{ih} und χ_{i0} auch von der thermisch-diffusen Streuung (TDS), der Compton-Streuung (CS) und der Plasmon-Streuung (PS) beeinflußt werden, blieben sie früher unberücksichtigt. Aus diesem Grund haben wir in Gl. (2) D_h' geschrieben; berücksichtigt man die Zusatzeffekte, so ist D_h' in D_h abzuändern.

Als Beispiele, bei denen die genannten Streueffekte nicht beachtet wurden, nennen wir die zumeist vor 1968 publizierten Arbeiten von Okkerse[1]; Batterman[2, 3]; Ling et al.[4]; Ludewig[5, 6]; Ghezzi et al.[7]. Sie befaßten sich mit der Temperaturabhängigkeit der anomalen Absorption von Röntgen-Strahlung in Germanium und hatten die Berechnung des Debye-Faktors und damit die Bestimmung der Debye-Temperatur zum Ziel. Die Größe $\varepsilon_0^{\perp}$ wurde theoretischen Rechnungen bezüglich des Photo-Effektes entnommen[8, 9]. Die genannten Autoren verglichen nach der Formel von Kato[10] berechnete Reflexintensitäten mit gemessenen Inten-